Biochimica et Biophysica Acta 1802 (2010) 443–453

Contents lists available at ScienceDirect

Biochimica et Biophysica Acta

journal homepage: www.elsevier.com/locate/bbadis

Mitochondrial bioenergetics and dynamics interplay in complex I-deficient fibroblasts

M. Morán [a,c], H. Rivera [a,c], M. Sánchez-Aragó [b,c], A. Blázquez [a,c], B. Merinero [b,c], C. Ugalde [a,c], J. Arenas [a,c], J.M. Cuezva [b,c], M.A. Martín [a,c,*]

[a] Centro de Investigación, Hospital Universitario 12 de Octubre, Madrid, Spain
[b] Centro de Biología Molecular Severo Ochoa, Consejo Superior de Investigaciones Científicas (CSIC-UAM), Madrid, Spain
[c] Centro de Investigación Biomédica en Red de Enfermedades Raras (CIBERER) U713, U723, U746 Madrid, Spain

ARTICLE INFO

Article history:
Received 29 July 2009
Received in revised form 3 February 2010
Accepted 8 February 2010
Available online 11 February 2010

Keywords:
Mitochondrial dynamics
Mitochondrial disease
NDUFA1
NDUFV1
Bioenergetics

ABSTRACT

Background: Complex I (CI) deficiency is the most frequent cause of OXPHOS disorders. Recent studies have shown increases in reactive oxygen species (ROS) production and mitochondrial network disturbances in patients' fibroblasts harbouring mutations in CI subunits. *Objectives*: The present work evaluates the impact of mutations in the *NDUFA1* and *NDUFV1* genes of CI on mitochondrial bioenergetics and dynamics, in fibroblasts from patients suffering isolated CI deficiency. *Results*: Decreased oxygen consumption rate and slow growth rate were found in patients with severe CI deficiency. Mitochondrial diameter was slightly increased in patients' cells cultured in galactose or treated with 2′-deoxyglucose without evidence of mitochondrial fragmentation. Expression levels of the main proteins involved in mitochondrial dynamics, OPA1, MFN2, and DRP1, were slightly augmented in all patients' cells lines. The study of mitochondrial dynamics showed delayed recovery of the mitochondrial network after treatment with the uncoupler carbonyl cyanide *m*-chlorophenyl hydrazone (cccp) in patients with severe CI deficiency. Intracellular ROS levels were not increased neither in glucose nor galactose medium in patients' fibroblasts. *Conclusion*: Our main finding was that severe CI deficiency in patients harbouring mutations in the *NDUFA1* and *NDUFV1* genes is linked to a delayed mitochondrial network recovery after cccp treatment. However, the CI deficiency is neither associated with massive mitochondrial fragmentation nor with increased ROS levels. The different genetic backgrounds of patients with OXPHOS disorders would explain, at least partially, differences in the pathophysiological manifestations of CI deficiency.

1. Introduction

Complex I (CI), the largest component of the respiratory chain, is the first entry point of electrons into the oxidative phosphorylation (OXPHOS) system, and catalyzes the transfer of two electrons from NADH to ubiquinone. One of the 14 CI catalytic subunits is the NDUFV1 protein, which is encoded by the *NDUFV1* gene. This protein contains the NADH-binding site and the primary electron acceptor FMN [1]. CI also includes at least 31 accessory proteins of yet poorly understood functions, one of which is an integral membrane protein known as MWFE or NDUFA1, encoded by the X-linked gene *NDUFA1* [2]. The NDUFA1 protein is essential for CI function in mammalian mitochondria as it plays a role in CI stability, synthesis of the catalytic mitochondrial-encoded ND subunits and in their incorporation into the complex [3–5]. It has been hypothesized that phosphorylation could be implicated in the regulation of the complex activity [6,7], NDUFA1 phosphorylation at serine 55 being one of the phosphorylation sites that could affect CI function [8].

Dysfunction of the respiratory chain is the most frequent inborn error of metabolism [9]. CI deficiency is responsible for 40% of the OXPHOS disorders [10]. Mutations in several subunits and CI assembly factors have been associated with CI deficiencies [for a review see 1,11,12]. Recent studies revealed increases in reactive oxygen species (ROS) production [13–15] and mitochondrial network disturbances in patients' fibroblasts harbouring mutations in CI subunits [16–19].

In fibroblasts and other cells, mitochondria form a reticulum where they experience continuous cycles of fusion and fission during proliferation [20] mediated by specific proteins, such as mitofusins 1 and 2 (MFN1, MFN2), OPA1 and dynamin related protein 1 (DRP1) [21]. Some fibroblast lines derived from OXPHOS-deficient patients display a decrease in the branching and length of mitochondrial tubules that could reflect compromised mitochondrial homeostasis; other cells show an outgrow of the overall mitochondrial network that may indicate a compensative phenomenon [22]. Although a

* Corresponding author. Centro de Investigación, Hospital Universitario 12 de Octubre. Avda. de Córdoba s/n. 28041 Madrid, Spain. Tel.: +34 91 390 8001; fax: +34 91 390 8544.
E-mail address: mamcasanueva@h12o.es (M.A. Martín).

0925-4439/$ – see front matter © 2010 Elsevier B.V. All rights reserved.
doi:10.1016/j.bbadis.2010.02.001

relationship between mitochondrial morphology alterations and OXPHOS disorders has been reported, the possible alterations and role of fission and fusion proteins in these diseases has been scarcely studied [23,24].

The aim of the present study was to evaluate the impact of mutations in *NDUFV1*, and *NDUFA1* genes on mitochondrial bioenergetics and dynamics by using patients' fibroblasts.

2. Material and methods

2.1. Subjects

Patient 1 (P1) is a boy suffering acidosis, leukoencephalopathy and epilepsy, and harbouring W51X and T423M mutations in the *NDUFV1* gene who reached 14 months of age. Patient 2 (P2) and patient 3 (P3) were two unrelated male patients presenting R37S and G8R hemizygous mutations in the *NDUFA1* gene, respectively [25]. These mutations were associated with developmental delay and myoclonic epilepsy (P2) and Leigh syndrome (P3). P2 has already reached 10 years of age, while P3 died at 14 months of age of cardiorespiratory arrest during a respiratory infection.

2.2. Cell culture and treatments

Fibroblasts were obtained from skin biopsies and cultured in DMEM (i) with high glucose (4.5 g/L) (DMEM-Glu), or (ii) with no glucose but containing galactose (4.5 g/L) supplemented with 10% fetal calf serum, penicillin 50 IU/mL and streptomycin 50 IU/mL (DMEM-Gal); for glycolysis inhibition, cells were maintained in (iii) DMEM-Gal with 40 mM deoxyglucose for 8 h. The three media employed also contained 2 mM glutamine and 100 mM pyruvate. Mitochondrial dynamics was studied by inducing mitochondrial network fragmentation after treatment with the uncoupler carbonyl cyanide *m*-chlorophenyl hydrazone (cccp) 10 μM, for 4 h, and a subsequent recovery period of 4 h as described by Guillery et al. [19].

2.3. Enzyme activities of mitochondrial respiratory chain complexes

Mitochondrial respiratory chain complexes were assayed in sonicated suspensions of cultured skin fibroblast according to established methods [26]. The enzyme activities were corrected by citrate synthase activity, a classical marker of cellular mitochondrial content.

2.4. ATP content measurements

Cellular ATP was extracted from cells grown in DMEM-Glu, DMEM-Gal and DMEM-Gal-grown cells incubated with 40 mM 2′-deoxyglucose for 4 h, in boiling 100 mM Tris, 4 mM EDTA pH 7.75, and assayed by bioluminescence using a luciferin–luciferase system (Roche) according to manufacturer's instructions. ATP concentration was corrected per mg of protein.

2.5. RT-PCR

Relative quantification of mtDNA versus nuclear DNA was performed by real-time PCR in a HT Real Time PCR System (Applied Biosystems, Foster City, CA, USA), using isolated DNA from control and patient's fibroblasts as described elsewhere [27].

2.6. Determination of aerobic glycolysis

For the determination of aerobic glycolysis cells were cultured in glucose; at the beginning of the experiment the culture media was replaced by fresh DMEM-Glu with or without 6 μM oligomycin; 2 h later, 0.1 mL aliquots of culture media were collected for the enzymatic determination of lactate [28].

2.7. Oxygen consumption

Oxygen consumption rate (OCR) in adherent fibroblasts was measured with a XF24 Extracellular Flux Analyzer (Seahorse Bioscience, Billerica, MA, USA). Control and patients' fibroblasts were seeded in XF 24-well cell culture microplates (Seahorse Bioscience) at 12.5×10^3 cells/well in 250 μL of DMEM-Glu or DMEM-Gal, and incubated at 37 °C/5% CO_2 for 24 h. Assays were initiated by replacing the growth medium from each well with 700 μL of unbuffered DMEM-Glu or DMEM-Gal prewarmed at 37 °C. The cells were incubated at 37 °C for 60 min to allow media temperature and pH to reach equilibrium before the first rate measurement. After an OCR baseline measurement, 50 μL of oligomycin (OL), carbonyl cyanide 4-(trifluoromethoxy)phenylhydrazone (FCCP), rotenone (RO) and nitropropionic acid (NPA) solutions were sequentially added to each well to reach working concentrations of 6 μM, 50 μM, 1 μM and 10 μM respectively, and changes in the OCR were analyzed.

Data were expressed as pmol of O_2 per minute per 10^6 cells and normalized by mitochondrial mass determined by flow cytometry (nonyl acridine orange, NAO, fluorescence arbitrary units). Maximal respiratory rate was calculated as the difference between the OCR after FCCP injection and the lowest OCR reached after rotenone addition. Oligomycin sensitive respiration rate (OSR) was calculated as the difference between the basal OCR and the OCR after oligomycin injection. OSR expressed as the percentage of the maximal respiratory rate in each cell line represents mitochondrial coupling.

2.8. Immunofluorescence microscopy

Immunofluorescence was performed on sub-confluent paraformaldehyde-fixed cells. Antigen retrieval, when needed, was performed by submerging the coverslips in 100 mM Tris pH 9.5, 5% urea for 10 min at 95 °C. Coverslips were PBS washed, and permeabilized for 15 min with 0.1% Triton X-100. Cells were incubated in blocking buffer containing 10% goat serum for 1 h at room temperature. The mouse monoclonal anti-complex V α subunit (MitoSciences), or anti-Porin (MitoSciences) were used as primary antibodies. Texas Red-conjugated anti-mouse (MitoSciences) was used as secondary antibody. After appropriate rinsing, coverslips were mounted in ProLong Gold antifade reagent (Molecular Probes) on glass slides and cells were viewed with a Zeiss LSM 510 Meta confocal microscope with a 63× planapochromat objective.

2.9. Analysis of intracellular ROS in live cells by confocal microscopy

Cells grown on coverslips were loaded with 5 μM 2′,7′-dichlorofluorescin diacetate (DCF-DA, Sigma) for 20 min in the dark in a CO_2 incubator. DCF-DA is a nonpolar and nonfluorescent compound, which diffuses into the cells and is hydrolyzed to polar 2′,7′-dichlorofluorescin, thereby trapped within the cells. Subsequently intracellular 2′,7′-dichlorofluorescin is rapidly oxidized to highly fluorescent 2′,7′-dichlorofluorescein in the presence of ROS or hydrogen peroxide in the cells [29]. After loading, the dye was removed and cells washed twice with PBS before image collection with a Zeiss LSM 510 Meta confocal microscope. The image collection was carried out with a 20× lens using the 488 nm excitation laser line. As positive control, human fibroblasts from patients suffering mitochondrial respiratory chain complex III deficiency producing significant amounts of ROS were analyzed in parallel.

2.10. Flow cytometry

The fluorescent probes NAO (Molecular Probes) and 2′,7′-dichlorofluorescin diacetate (DCF-DA, Sigma) were used to analyze cardiolipin, as a marker of cellular mitochondrial content, and ROS production respectively, using flow cytometry. The cellular fluorescence intensity was measured using a FACScan flow cytometer (Beckton-Dickinson). For each analysis 10,000 events were recorded.

2.11. Western blot analysis in cell lysates

Fibroblasts grown either in DMEM-Glu or DMEM-Gal were lysated in 5 mM Tris pH 8.0, 20 mM EDTA, 0.5% Triton X-100 and 100 μg/mL of protease inhibitors, centrifuged at 11,000×*g*, and supernatant was collected. Protein content of the supernatants (cell lysates) was determined [30]. Samples of cell lysates (10 μg) were used to perform semiquantitative analysis of DRP1, MFN2 and OPA1 protein levels by immunoblotting (Western Blot). SDS-PAGE was performed on a 7.5% separation gel for proteins involved in fusion and fission, whereas 15% and 12% separating gels were used for western blot analysis of GAPDH and antioxidant enzymes, respectively. Resolved proteins were transferred to a PVDF membrane. Blots were blocked and incubated with the following primary antibodies: mouse anti-DLP1 (BD Transduction Laboratories™), mouse anti-OPA1 (BD Transduction Laboratories™), mouse anti-MFN2 (Abnova), anti-GAPDH (Abcam), rabbit anti-mtSOD (mitochondrial superoxide dismutase, Sigma), mouse anti-CAT (catalase, Sigma) and rabbit anti-GR (gluthathione reductase, Abcam). Immunodetection of primary antibodies was carried out with peroxidase-conjugated goat anti-mouse antibody (Molecular Probes). The signal was detected with Enzyme Chemiluminescence (Amersham Biosciences). Band densities were evaluated by densitometric scanning (Image J software). To verify that the total protein amount loaded in each lane was the same, β actin or α tubulin were immunodetected with mouse anti-β actin or anti-α tubulin (Sigma) coupled to peroxidase-conjugated goat anti-mouse antibody (Molecular Probes).

2.12. Data analysis

All determinations were performed at least in duplicate. Data are presented as mean ± standard deviation (SD). Statistical analysis was performed with the SPSS software (SPSS, Chicago, IL). Mean NAO fluorescence and mtDNA content of $n = 3$–8 samples are presented; to analyze the group effect on these parameters a Kruskal–Wallis test was performed, with statistical significance set at $P \leq 0.05$. Immunofluorescence photographs were analyzed with Image J software (http://rsbweb.nih.gov/ij/). Mitochondrial diameter was determined as follows: after calibrating the images according to the objective employed to obtain the photographs, the mitochondrial width was measured with Image J software; results were presented as mean (±SD) values of 200 determinations. In the present work 4 control cell lines were analyzed. For every condition tested, the width of 200 mitochondria in 10 cells representative of the mitochondrial morphology was determined. To analyze ATP concentration, extracelullar lactate levels and mitochondrial diameter in fibroblasts grown in different culture media, we performed a two-way ANOVA that allowed us to assess the two main effects, i.e. group (control or patient) and treatment (−OL/+OL) or growth medium (DMEM-Glu, DMEM-Gal or Gal + Deoxyglucose), as well as the interaction

Table 1
Activities of the mitocondrial respiratory chain enzymes in fibroblasts derived from the patients.

	CS	CI	CII	CIII	CIV
Glucose					
Control ($n = 5$)	66–94	21.6–34.7	12.8–27.4	31.1–50.9	89–120
P1	77	**7.7**	23.6	48.7	**86**
P2	87	**19.0**	25.3	39.7	**123**
P3	**106**	**8.8**	16.4	32.6	91.4
Galactose					
Control ($n = 5$)	72–84	21.0–28.4	19.0–29.4	20.8–45.2	104–123
P1	63	**9.6**	27.3	**54.0**	**149**
P2	81	**18.8**	27.3	42.4	**141**
P3	**109**	**9.54**	**14.8**	30.4	107

Abnormal values are indicated in boldface.
Enzyme activities are expressed in cU/U CS.
Citrate synthase (CS) activity is expressed as nmol min^{-1} mg^{-1}.

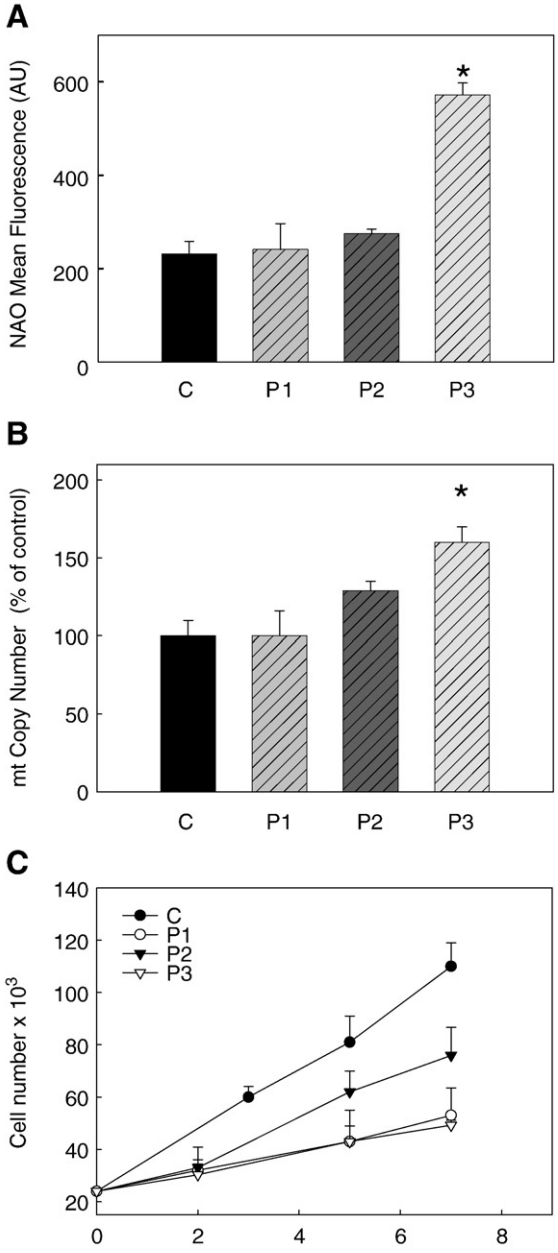

Fig. 1. Mitochondrial mass and growth rate in galactose. A) Flow cytometry determination of mitochondrial mass in control (C) and patients' skin fibroblasts (P1, P2, P3) stained with NAO probe. *$P<0.05$ for P3 *vs* rest of cells lines. B) Relative quantification of mtDNA *vs* nuclear DNA by real-time PCR, data are presented as percentage of controls. *$P<0.05$, for P3 *vs* the rest of the cell lines. C) Mean growth rates in DMEM-Gal. Data are presented as mean value ± SD ($n = 3$).

(group*treatment/medium) effect. To analyze the effect of cccp treatment on mitochondrial diameter we used a two-way ANOVA with repeated measures that allowed us to test the two main effects (group and treatment) and the group*treatment interaction effect. The Scheffé test was employed *post hoc* to determine the differences between groups. A level of $P \leq 0.05$ was selected to indicate statistical significance.

3. Results

As expected, all the fibroblast lines derived from the patients showed decreased CI activity in both DMEM-Glu and DMEM-Gal media (Table 1). In DMEM-Gal medium the range of CII and CIV activities shifted toward higher values in the control fibroblasts. In the patients' cells grown in DMEM-Gal a slight increase in CI activity was detected in P1 and P3 cells in comparison with glucose-grown cells. Also, in DMEM-Gal the activities of CII and CIII were augmented in P1 and P2, and CIV activity was increased in the three patients. These results, that reflect an adaptation to this metabolic environment, correlate with previous data showing augmented expression levels of some respiratory chain subunits in galactose-grown fibroblasts [31]. The CS activity, an indicator of cellular mitochondrial content, was slightly increased in P3 in both culture media (Table 1). Flow cytometry analysis showed a marked increase in cardiolipin in P3 ($P<0.05$) (Fig. 1A); mtDNA content determination by real-time PCR also indicated a significant increase in mtDNA in P3 ($P<0.05$) (Fig. 1B). The results obtained by these three approaches support the presence of an increased mitochondrial content in P3.

When cells are grown in DMEM-Gal, galactose enters slowly the glycolysis [32], and in such condition, patients' fibroblasts showed a strong reduction in growth rate compared with control cells, with the mildest decrease being observed in P2 (Fig. 1C). A milder decrease in growth rate was also detected in the patient's fibroblasts cultured in DMEM-Glu (data not shown).

3.1. Mutations in CI alter mitochondrial bioenergetics

The XF24 Extracellular Flux Analyzer allows determination of OCR in adherent cells [33]. In order to determine oligomycin sensitive respiration, maximal respiration, and oxygen consumption due to CI and complex II activity, OL, FCCP, RO and NPA were sequentially added to the attached cells (Fig. 2). The qualitative analysis of the results obtained showed that all cell lines displayed similar bioenergetic profiles in DMEM-Glu (Fig. 2A) and DMEM-Gal (Fig. 2B). After OL injection OCR was decreased, and maximal respiratory rate was achieved after FCCP addition. The basal respiratory rates observed in the present work are half of the maximal ones, according to previous data obtained in human fibroblasts by Gnaiger et al. [34]. Rotenone treatment induced a strong decrease in OCR, setting the respiration near zero values, and therefore, NPA addition was unable to induce a

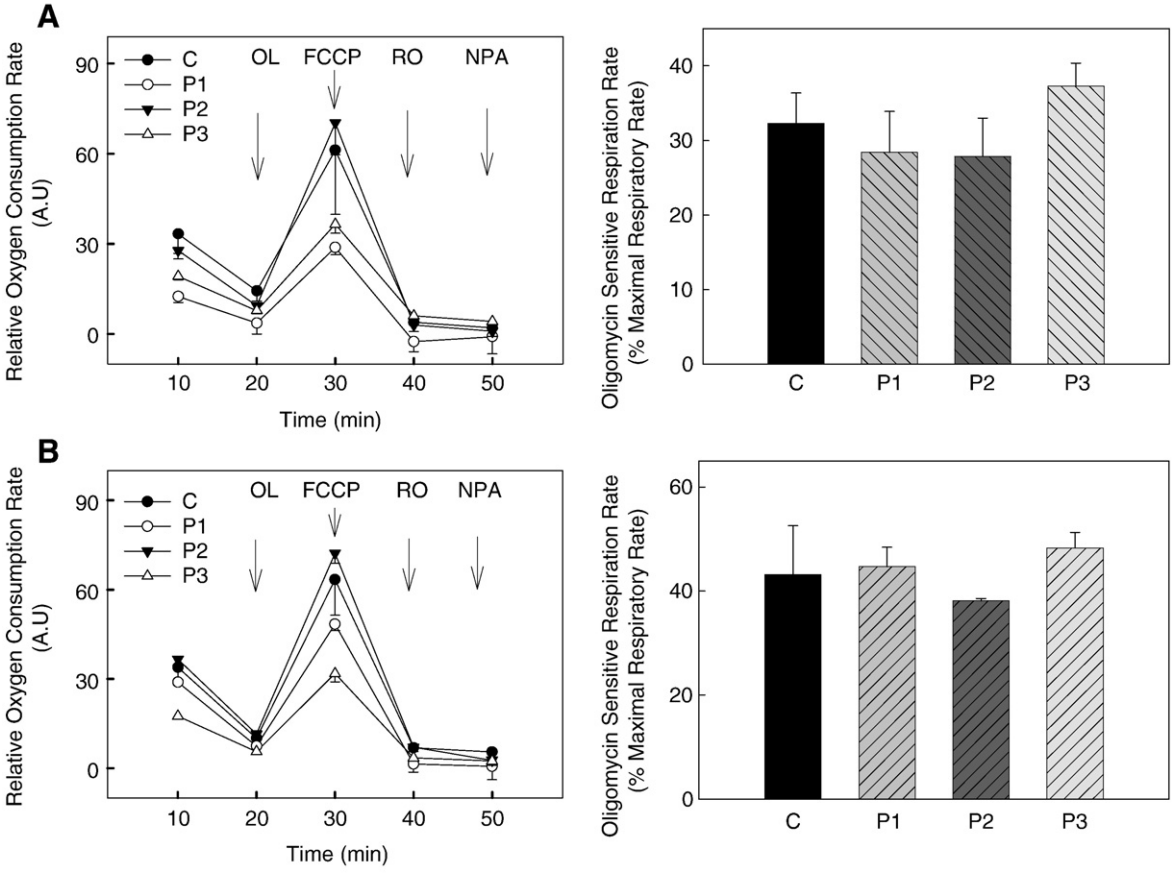

Fig. 2. Oxygen consumption. Real-time analysis of oxygen consumption rate (OCR) in control (C) and patients' cells (P1, P2, P3) determined with XF24 Extracellular Flux Analyzer in cells respiring in DMEM-Glu (A) and DMEM-Gal (B). Oligomycin (OL), FCCP, rotenone (RO) and nitropropionic acid (NPA) were injected sequentially at the time points indicated by arrows into each well containing 12,500 cells after baseline measurements. Data are expressed as pmol of O_2 per minute per 106 cells, and normalized per units of mitochondrial mass as assessed by NAO fluorescence. Basal OCR in controls respiring in DMEM-Glu was 96.7 ± 19 (pmol O_2/min/12,500 cells), $n = 8$. Oligomycin sensitive respiration rate, which represents oxidative phosphorylation rate, was calculated as percentage of maximal respiratory rate.

further decrease in OCR (Fig. 2). According to recent data [34], the inhibition of CI by rotenone may increase the cellular NADH/NAD^+ ratio, leading to inhibition of α-ketoglutarate dehydrogenase activity and, subsequently succinate production. This phenomenon would stall CII activity, and thus might explain the strong inhibition of respiration in adherent cells treated with rotenone that we observed in the present study.

In DMEM-Glu, P1 and P3 showed decreased basal and maximal OCR, whereas P2 presented normal values in comparison with control cells (Fig. 2A). When cells were respiring in DMEM-Gal, basal and maximal OCR did not change in control fibroblasts in comparison with DMEM-Glu conditions (Fig. 2B). In P1, the basal and maximal OCR increased with DMEM-Gal, but still remained below control values. A slight increase in basal OCR was shown in P2, although maximal OCR did not change. Finally, P3 fibroblasts were unable to increase their basal and maximal OCR in DMEM-Gal, and remained significantly below control values.

Oligomycin sensitive respiration rate (OSR) represents the activity of oxidative phosphorylation (Fig. 2), that is, the synthesis of ATP by complex V coupled to the activity of the respiratory chain. When expressed as percentage of maximal respiratory rate, OSR represents the degree of mitochondrial coupling. Control and patients' cells showed a similar degree of mitochondrial coupling, which indicates that patients' fibroblasts did not suffer any alteration in oxidative phosphorylation. Nevertheless, the diminished basal OCR shown in P1 and P3 (37% and 58% of the control value respectively) may have induced a reduction in ATP synthesis by OXPHOS system in these cells lines. When cultured in DMEM-Gal, all the cell lines experienced an increase in OSR (mean OSR in glucose 31.5 ± 4 *vs* 43.6 ± 4 in galactose), reflecting increased mitochondrial coupling and, as expected, increased ATP synthesis through the OXPHOS system.

ATP content was significantly decreased in all patients' cells grown in glucose, in comparison with control fibroblasts, a further decrease in this parameter was detected in galactose-grown P1 and P3 cells ($P<0.001$) (Fig. 3A). Treatment with 2′-deoxyglucose induced a marked decrease in ATP content in all cell lines, including fibroblasts; this result suggests that, even in DMEM-Gal, glycolysis is contributing to ATP production in all cell lines.

To assess the contribution of glycolysis to the ATP production in DMEM-Glu, glycolytic flux was estimated by lactate release (Fig. 3B). Only P3 showed an increased basal lactate production rate in DMEM-Glu ($P<0.001$) (Fig. 3A) when compared to control or other patients, strongly suggesting the pathogenicity of the *NDUFA1* mutation in cellular bioenergetics [35,36]. The rates of glycolytic flux after OL treatment were marginally affected in the different cell lines ($P>0.05$ for OL treatment) (Fig. 3B), indicating that glycolysis was running at maximal capacity in all cell lines. In agreement with this finding, the expression levels of GAPDH, a key enzyme of the glycolytic pathway, were not altered in patients' cells in comparison with control fibroblasts (Fig. 3C).

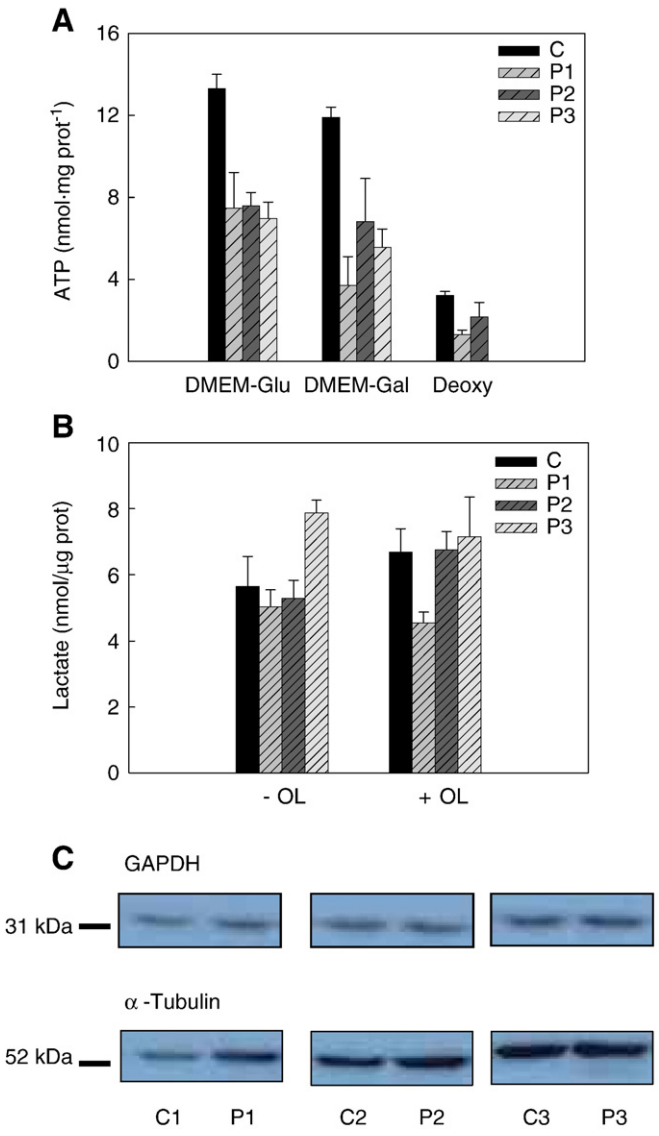

Fig. 3. ATP levels and Glycolytic flux. A) Cellular ATP content in control (C) and patient's cell grown in DMEM-Glu, DMEM-Gal and cells after 4 h incubation with galactose medium with deoxyglucose (Gal + Deoxyglucose). Two-way ANOVA analysis: significant main effect for group ($P<0.001$), treatment ($P<0.001$) and interaction between them ($P<0.001$). Glycolytic flux estimated by lactate release to the extracellular medium. B) Lactate levels in DMEM-Glu culture medium of fibroblasts nontreated (−OL) and treated with oligomycin (+OL). Two-way ANOVA analysis: significant main effect for group effect *($P<0.05$). C) Expression levels of the key glycolytic enzyme, GAPDH, and loading control with α-tubulin, in control (C), and patients' cells (P1, P2, P3) cultured in high glucose medium.

3.2. CI deficiency promotes a delay in mitochondrial network recovery

The transversal section (width) of a mitochondrion is the most stable dimension of this organelle and variations in this variable reflect an alteration of the mitochondrial morphology [37]. When cells are grown in DMEM-Glu, mitochondrial network in control fibroblasts is composed of long branched mitochondrial filaments (Fig. 4A) and overall mitochondrial morphology in nonsynchronized cultures is similar to that observed in G_0-arrested cells (data not shown). Under this condition, patients' cells showed essentially a normal mitochondrial architecture and mitochondrial width; yet in P3 an increased mitochondrial content was observed, which is consistent with the increased mitochondrial mass shown by flow cytometry and real-time PCR (Fig. 1). When glucose was substituted by galactose, both control and OXPHOS defective fibroblasts were able to maintain normal mitochondrial morphology (Fig. 4A) and only a slight increase in mitochondrial diameter was found in all cell lines (Fig. 4B). In order to force cells to rely only in respiratory chain to obtain energy, cells were maintained in DMEM-Gal with 2′-deoxyglucose, a potent inhibitor of glycolysis. Although some abnormal structures appeared in the presence of deoxyglucose, most of the cells were able to maintain a normal mitochondrial architecture (Fig. 4A) and the mitochondrial diameter was slightly augmented as in DMEM-Gal (Fig. 4B).

A slight increase in the main proteins implicated in mitochondrial fusion and fission, OPA1, and DRP1, was observed in the patients' cells under glucose conditions (Fig. 5). When fibroblasts were cultured in DMEM-Gal, increases in OPA-1 and MFN2 were found in both P2 and P3, and DRP1 levels were increased in the three patients. In the two culture conditions analyzed, DMEM-Glu and DMEM-Gal, the long isoforms of OPA1 were predominant in both control and patient's cells.

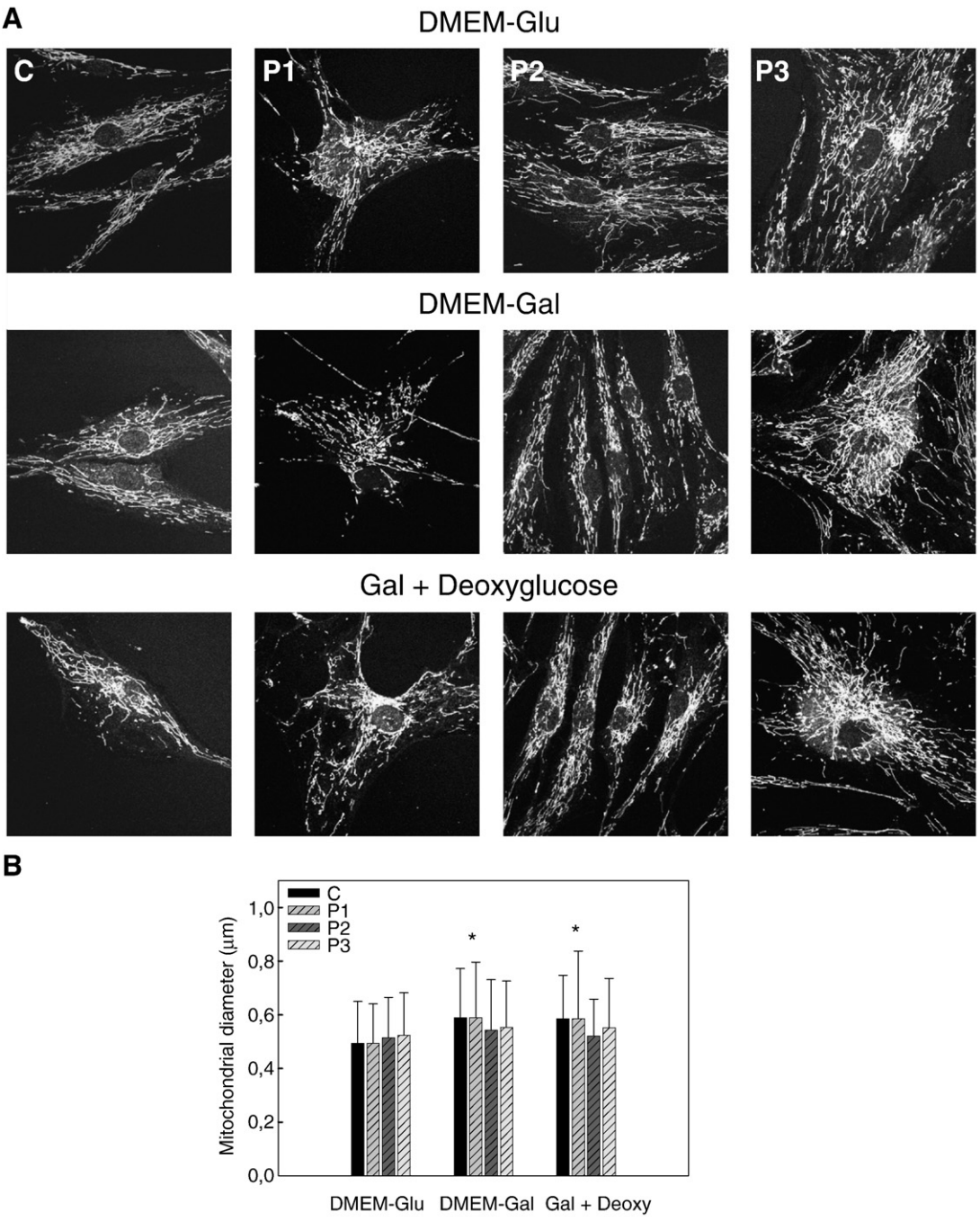

Fig. 4. Mitochondrial network morphology. A) Typical mitochondrial network morphology in control (C), patient's skin fibroblast (P1, P2, P3) grown in high glucose medium (DMEM-Glu), galactose medium (DMEM-Gal) and after 8 h in galactose medium with deoxyglucose (Gal + Deoxyglucose). Cells were fixed with paraformaldehyde and immunofluorescence against complex V alpha subunit was performed. B) Mitochondrial diameter in DMEM-Glu grown fibroblasts (Glucose), DMEM-Gal grown fibroblasts (Galactose) and after 8 h in galactose with deoxyglucose medium (Galactose + D). The results shown are the means ± SD of 200 determinations. Two-way ANOVA analysis: significant main effect for group ($P<0.001$), treatment ($P<0.001$) and interaction between them ($P<0.001$). *($P<0.001$) significantly different from DMEM-Glu diameter.

Mitochondrial dynamics in CI defective fibroblasts was analyzed in cells treated with cccp as described by Guillery et al. [19] (Fig. 6A). After 4 h of treatment with the protonophore, control and patients' cells displayed a marked mitochondrial fragmentation that resulted in a significant increase in mitochondrial diameter (Fig. 6B). This result demonstrates efficient mitochondrial fission in the three patients. After a 4-hour recovery period in fresh medium devoid of cccp, control and P2 cells almost recovered the previous mitochondrial tubular network, but P1 and P3 showed significantly increased mitochondrial diameter that reflected a delay in the recovery of their initial mitochondrial morphology ($P<0.001$).

3.3. ROS production

The ROS levels in living fibroblasts were estimated as DCF-DA fluorescence using confocal microscopy (Fig. 7A). In control and patients' cell lines fluorescence levels in fluorophore-loaded cells cultured in both DMEM-Glu and DMEM-Gal were similar to those detected in non-loaded fibroblasts. This result demonstrates that basal DCF-DA detectable ROS levels were below the detection limit in both control and patients cells. Flow cytometry analysis of ROS production in cells respiring in DMEM-Glu, confirmed the results obtained with confocal microscopy, as no differences between

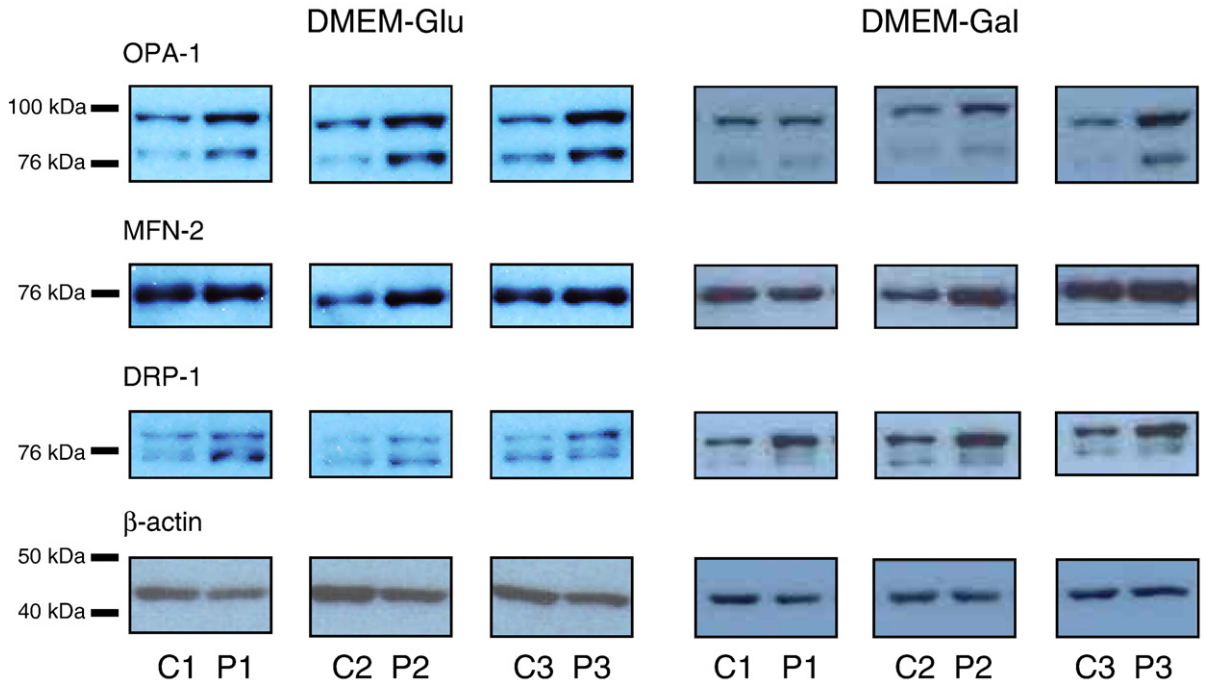

Fig. 5. Expression levels of fusion and fission proteins. Expression levels of OPA-1, MFN2, DRP1 of fibroblast grown in DMEM-Glu and DMEM-Gal determined by Western blotting as described in Materials and methods. β-actin was used as a loading control.

patients and control cells were found (Fig. 7C). To study the levels of the cellular antioxidant defences, we analyzed the expression levels of some of the main antioxidant enzymes in glucose-grown cells (Fig. 7D). The results obtained showed a significant increase in mtSOD levels only in P2, whereas, CAT and GR expression levels were within the control range in all patients' cell lines.

4. Discussion

Our main finding was that severe CI deficiency in *NDUFA1* and *NDUFV1* mutant patients is linked to a delayed mitochondrial network recovery after cccp treatment. However, the CI deficiency is neither associated with massive mitochondrial fragmentation nor with increased ROS levels. The different genetic backgrounds of patients with OXPHOS disorders would partially explain the differences in the pathophysiological manifestations of CI deficiency. There were several novel aspects in our investigation. To date only three *NDUFA1* human mutants have been reported [25,38] and no functional study has been performed in human cell lines derived from these patients. Potlury et al. [38] recently analyzed the effects of the *NDUFA1* mutations reported here in a hamster cell line. On the other hand, only two *NDUFV1* mutants have been studied with discrepancies in the findings concerning mitochondrial morphology and ROS production [39].

The bioenergetic analysis with the XF24 Extracellular Flux Analyzer demonstrated those patients with more severe CI deficiency had decreased basal and maximal OCR, a finding that correlates well with their worse clinical courses (P1 reached 14 months of age and P3 died at 14 months, whereas P2 reached 10 years of age) and growth rate. The efficiency of oxidative phosphorylation was unaffected in the patients, which is in accordance with previous research by Caissereau et al. [40], reporting no alterations in OXPHOS coupling in CI-deficient fibroblasts harbouring mutations in *GDAP1*.

Mitochondria are dynamic organelles undergoing continuous cycles of fusion and fission especially visible during proliferation [20]. The equilibrium between these two opposite processes defines the overall architecture of the mitochondrial network in healthy cells. Alterations in mitochondrial morphology have been recently linked to several mitochondrial diseases, supporting the relationship between energy production and mitochondrial morphology [16–19]. It has been proposed that CI deficiency and the degree of mitochondrial complexity (mitochondrial length and branching) could be mutually dependent phenomena [10]. Large reductions in CI activity have been associated with a decrease in mitochondrial mass and/or enhanced fission, whereas moderate deficiencies have been linked with increased mitochondrial mass [10,39]. In the present work, P1 and P3 showed a severe and more pronounced decrease in CI activity than P2 (36% and 41% *vs* 88% of the lowest control value, respectively) but no evidence of mitochondrial fragmentation. On the contrary, increased mitochondrial content composed by long tubular mitochondria was shown in P3. Other authors also described fibroblasts from patients suffering severe CI deficiency, yet exhibiting filamentous mitochondrial morphology [19,41]. In addition, two patients harbouring the same mutations in *NDUFV1* and a similar degree of CI deficiency displayed opposite mitochondrial morphologies [10,39]. These results suggest that low residual CI activity is not always associated with a fragmented mitochondrial network. The different genetic background in each CI-deficient patient, e.g. genes that mediate compensatory mechanisms or genes encoding other OXPHOS subunits, could affect the pathophysiological phenotype found in patients' cells. Such interactions could partially explain discrepant observations of mitochondrial morphology among studies or even between patients harbouring the same mutations. In this regard, Potlury et al. [38] recently suggested that synergistic interactions between mtDNA and nDNA encoded subunits of the OXPHOS system, affect CI defects. This phenomenon could be of great importance in *NDUFA1* mutants, as the NDUFA1 protein is known to interact with several mitochondrial-encoded ND subunits [4]. Finally, different methodological approaches, i.e. culture media, could also explain, partially discrepancies between studies.

It has been described that under basal culture conditions with high glucose availability, fibroblasts obtain most of the energy from glycolysis [19,31]. Our data support this hypothesis because, in DMEM-Glu, glycolysis is running at its maximal capacity. In the patients' cells, where glycolysis was also working actively, the decreased levels of ATP suggest that some energy consuming process was operating. When respiratory chain is inhibited, e.g. by rotenone, the F_1F_0-ATPase starts to function as a proton pump and hydrolyses

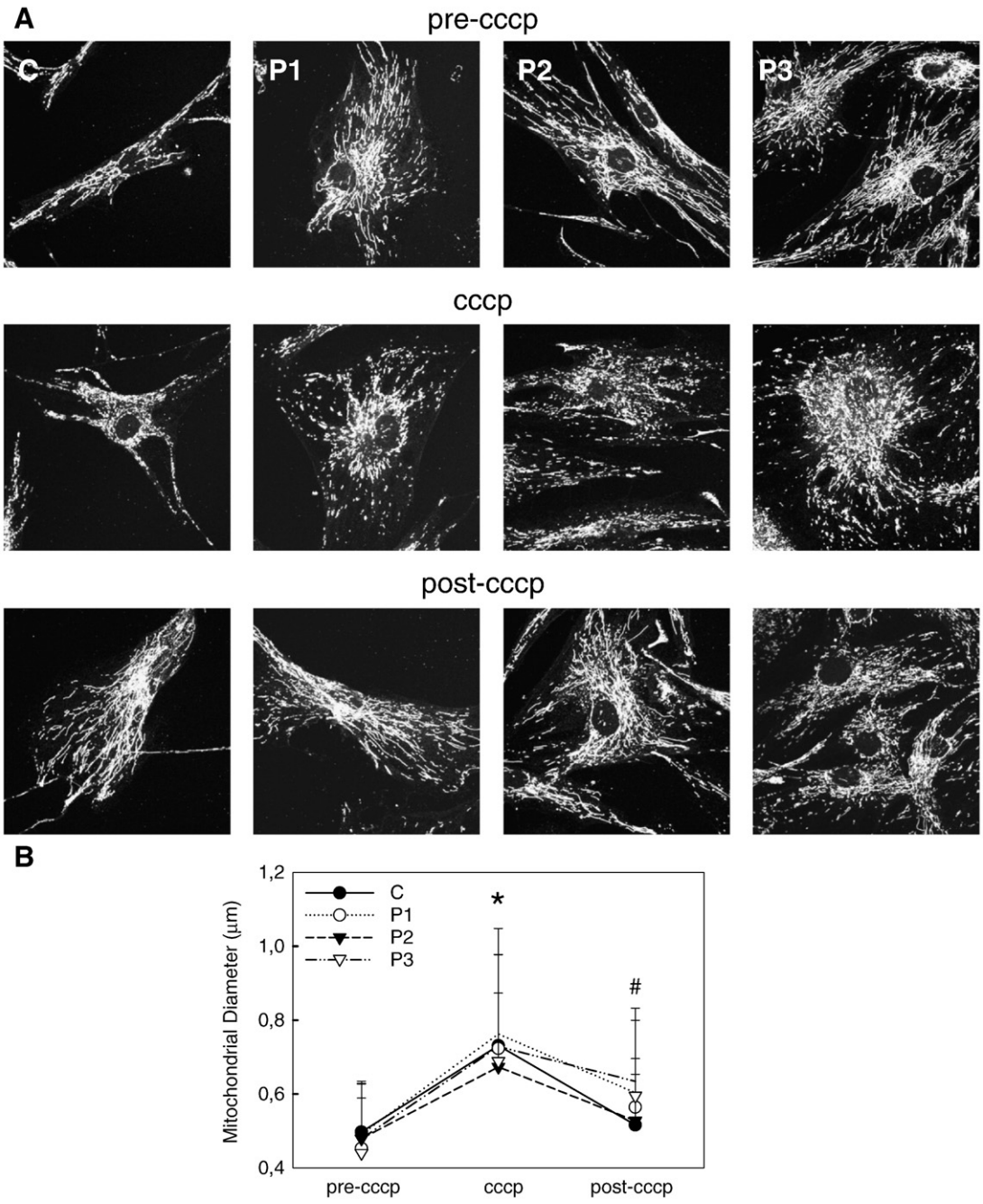

Fig. 6. Mitochondrial dynamics. A) Mitochondrial morphology in control (C) and patients' skin fibroblasts (P1, P2, P3) not treated (pre-cccp), treated with 10 μM cccp (cccp) and after 4 h of cccp wash out (post-cccp). Cells were fixed and immunofluorescence against porin was performed. B) Mitochondrial diameter in the above mentioned groups. The results shown are the means ± SD of 200 determinations. Two-way ANOVA analysis: significant main effect for group ($P<0.001$), treatment ($P<0.001$) and interaction between them ($P<0.001$). *($P<0.01$) P1 *vs* P2. #($P<0.001$) for significant differences between P3 and the remaining groups.

glycolysis-derived ATP, to prevent a decrease in mitochondrial membrane potential [for a review see 42]. Interestingly, Potlury et al. reported increased expression levels of complex V in the other *NDUFA1* mutant described so far [38], and preliminary data from our laboratory indicated that complex V alpha and beta subunits were also overexpressed in P1 and P3. These results could suggest that in the patients under the current investigation the reverse operation of ATPase could be consuming glycolysis-derived ATP to maintain mitochondrial membrane potential, leading to decreased ATP levels and growth delay. This situation would be further aggravated in DMEM-Gal, where glycolysis is running at a lower rate. Studies investigating this possibility are underway in our laboratory.

It has been described that when cells are grown in a culture medium devoid of glucose, galactose enters slowly the glycolysis [32,43]; this approach has been used to force the skin fibroblasts derived from mitochondrial diseased patients to get ATP through the OXPHOS system [44–46]. In the present work a slight decrease in ATP levels was detected in control and P2 cell lines grown in galactose, as well as significant decreases in P1 and P3. In control and patients' cells grown in galactose, we also observed an increase in mitochondrial coupling, in some respiratory chain activities, and in mitochondrial diameter, as an adaptation to this new metabolic environment. The reason of the slight increase in mitochondrial diameter we observed in cells grown in DMEM-Gal is not clear, but could be related to an

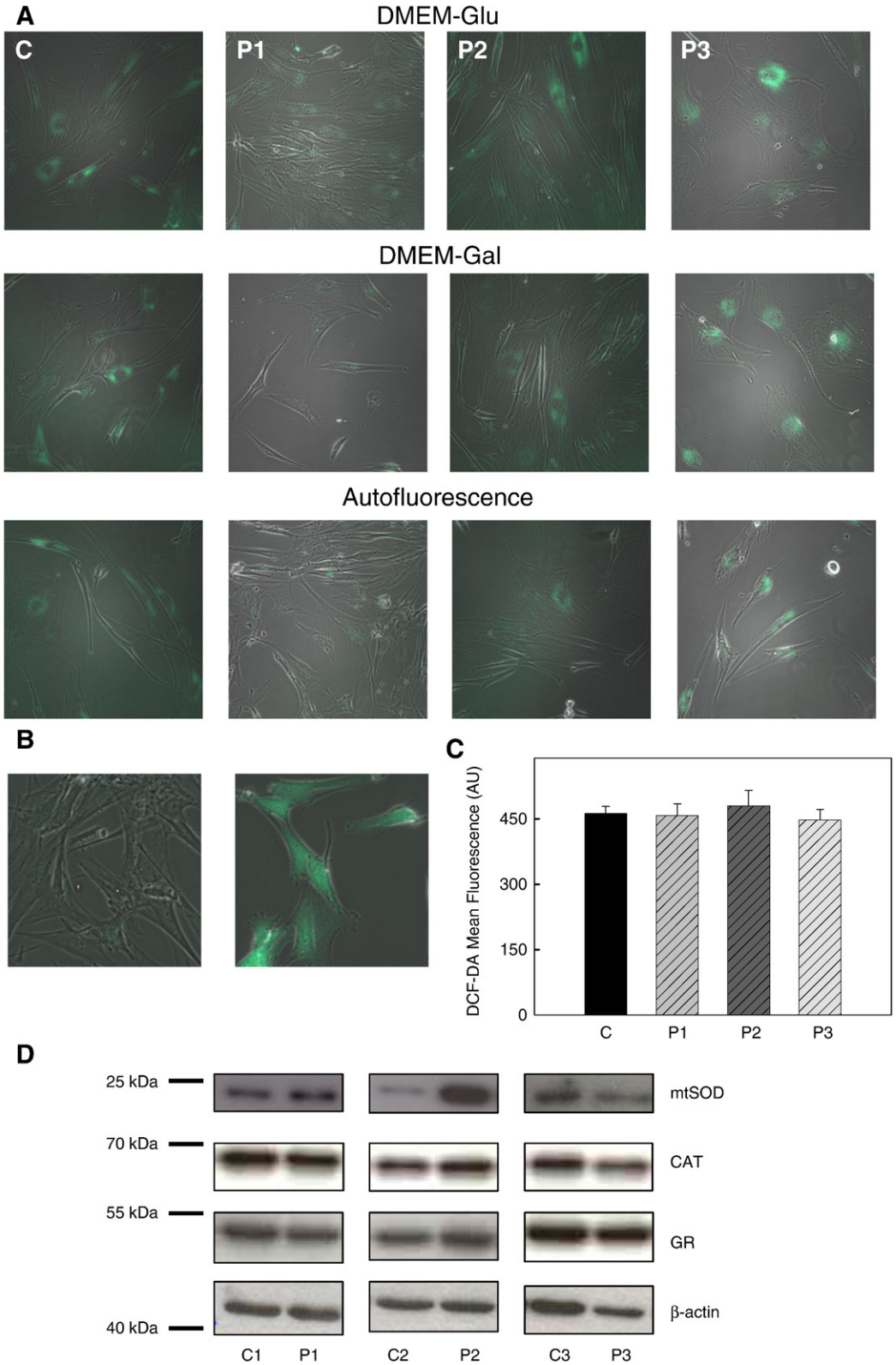

Fig. 7. ROS levels in control and patients cell lines. A) Confocal images of intracellular ROS generation (green fluorescence) merged with contrast-phase images from control (C), and patient's fibroblast (P1, P2, P3) cultured in high glucose DMEM (DMEM-Glu) or in galactose DMEM (DMEM-Gal). Cells were preloaded with DCF-DA to capture the generated ROS. The confocal images represent a randomly chosen field after 3 days of cell culture under the various experimental conditions. In each cell line a group of cells were not loaded with DCF-DA to set the basal level of autofluorescence. B) Human fibroblasts from a patient suffering complex III deficiency non-DCF-DA loaded (left image) and DCF-DA-loaded showing increased ROS levels (right image). C) Flow cytometry determination of ROS production in DMEM-Glu grown cells with DCF-DA probe. D) Western blot analysis of mitochondrial superoxide dismutase (mtSOD), catalase (CAT) and glutathione reductase (GR) expression levels in control (C) and patients' (P1, P2, P3) cells. β-actin was used as a loading control.

adaptation to the lower glycolytic flux. Changes in mitochondrial diameter have been reported to be associated with different metabolic shifts [47]. For instance, the mitochondrial diameter of INS-1E cells was augmented when glucose content was decreased in the culture media [48]. Guillery et al. [19] reported massive mitochondrial fragmentation in cells undergoing severe OXPHOS disorders by glycolysis inhibition with 2-deoxyglucose. Our results do not agree with this previous report, as P1 and P3 suffered a severe CI deficiency but did not show significant fragmentation under 2-deoxyglucose treatment. Only an increase in mitochondrial diameter was detected in control and P1 cell lines. This augmented mitochondrial diameter might reflect a change in the metabolic state similar to that seen in the fibroblasts grown in DMEM-Gal, when glycolysis-derived ATP is limited. Finally, the lack of massive mitochondrial fragmentation in cell lines with marked OCR decrease under metabolic conditions that limits the amount of glycolysis-derived ATP (i.e., DMEM-Gal or 2-deoxyglucose treatment), supports the idea postulated by Guillery et al. [19] that mitochondrial membrane potential is more relevant for mitochondrial morphology than ATP levels.

Mitochondrial network morphology is the result of fusion and fission events that allow the cell to maintain a healthy, homogeneous mitochondrial population [21], i.e. by exchanging mitochondrial components and eliminating non-functional mitochondria [49]. The increased levels of OPA1 and DRP1 found in our patients' fibroblasts might reflect a compensatory cellular mechanism to enhance complementation and recycling of less functional mitochondria. The long isoforms of OPA1 were predominant in both control and patients' cells respiring in glucose and galactose conditions. This finding is in accordance with a recent study by Guillery et al. [24] that demonstrated a predominance of long OPA1 isoforms in CI-deficient fibroblasts. Mitochondrial membrane potential is the main modulator of OPA1 isoforms [24] and possibly of mitochondrial morphology (more so than ATP levels) [19]. Provided that our patients' cell lines displayed a predominance of long OPA1 isoforms and no significant mitochondrial fragmentation/uncoupling, we could hypothesize that patients' cells were able to maintain mitochondrial membrane potential in spite of their respiratory chain alteration. In support of this hypothesis, preliminary data from our laboratory indicated that mitochondrial membrane potential in basal culture conditions (high glucose) was not decreased in our patients (data not shown). Slight decreases in mitochondrial membrane potential have been described by Distelmaier et al., in ten cell lines of their 21 patient's cohort [50]. Nevertheless, Distelmaier et al. had previously reported alterations in mitochondrial morphology in some of these patients that could be due to their decreased membrane potential. Also, discrepancies between Distelmaier's data and the present work could be attributed to the different technical approach to measure mitochondrial membrane potential. Finally, the elevated MFN2 levels shown in P2 and P3 cells cultured in DMEM-Gal may represent a further attempt to compensate for the OXPHOS deficiency, i.e. by increasing mitochondrial fusion and complementation in such metabolic stressing conditions.

To test the fission and fusion efficiency in our patients' cells, we studied the kinetics of cccp-induced fragmentation and the recovery of the mitochondrial reticulum as described by Guillery et al. [19]. The cccp treatment led to a massive mitochondrial fragmentation that caused a significant increase in mitochondrial diameter in both control and CI-deficient cells. This result indicates that the fission machinery is efficient in the pathological cell lines, as previously reported in different OXPHOS-deficient fibroblasts [19]. The delay observed in mitochondrial tubule formation in P1 and P3 after treatment suggests a mild alteration in the mitochondrial fusion process. The decreased OCR in these two patients reflects a low electron flux through the respiratory chain, which could in turn result in a delayed recovery of the mitochondrial membrane potential after the cccp treatment. Because mitochondrial membrane potential is required for efficient fusion [51] a delayed restoration of this parameter could induce a subsequent delay in the recovery of mitochondrial morphology after cccp treatment; yet, this hypothesis remains to be elucidated.

ROS production can increase in fibroblasts from CI-deficient patients, with larger increases being found in the more severe CI deficiencies [13–15]. In the present work none of the patients' cells lines showed increased ROS levels. One of the factors that determines the rate of $O_2^{\cdot-}$ production by mitochondria is the concentration of enzymes/proteins containing electron carriers that can react with O_2 to form $O_2^{\cdot-}$ [52]. Together with complex III, CI is one of the mitochondrial sites responsible for ROS production. Given that our *NDUFA1* mutants presented decreased levels of fully-assembled CI [25], a hypothetic increased ROS production due to abnormal function of respiratory chain, could be counteracted by the lowered CI levels. This would explain the normal ROS levels found in these two patients. Nevertheless, significant amounts of ROS have been described in fibroblasts with decreased CI levels [50]. Another possibility is that an increased antioxidant defence in the patient's cells could have counteracted the increased ROS production. Yet, in the present work only P2 cells showed augmented expression levels of mtSOD, with the other key antioxidant enzymes remaining unchanged. Although in this patient the increase in mtSOD could suggest an increase in ROS production, increases in antioxidant defences cannot explain, as a general rule, the absence of increases in ROS levels in the present study. Moreover, Verkaart et al. [14,15] studied ROS production in two patients harbouring mutations in the *NDUFV1* gene, finding increased ROS levels in one case and no alterations in the other mutant. The effect of *NDUFV1* mutations, and in other CI subunits, on ROS production would depend on several factors such as: their effects on NADH binding and NADH oxidation by FMN, the electron flux through the complex, or the interactions between the mutated and other CI subunits. Therefore, opposite effects in ROS production of different mutations are possible. Further mechanistic studies are needed to unravel their impact on ROS production.

In conclusion, severe CI deficiency in patients harbouring mutations in the *NDUFA1* and *NDUFV1* genes is linked to a delayed mitochondrial network recovery after cccp treatment, but not to massive mitochondrial fragmentation or to increased ROS levels. These results suggest that the different genetic backgrounds of patients with OXPHOS disorders might play a role in the pathophysiologic manifestations of the mutations.

Acknowledgements

We thank Alejandro Lucía for his helpful advice on revision of the manuscript, and Begoña Santiago for her kind support with the confocal microscope. This work was supported by grants PI060547 (to M.A.M.) from Instituto de Salud Carlos III (ISCIII), Ministry of Science and Innovation (MICIN), BFU 2007-65253 from the Ministry of Education and Science, and GEN-0269/2006 from Comunidad de Madrid (CM) (to M.A.M. and J.M.C.), Spain. M.M. is recipient of a post-doctoral fellowship from ISCIII (CD06/00031). H.R. is supported by the grant PI060547 (ISCIII). C.U. is recipient of a "Miguel Servet" research contract from ISCIII (CI04/00011). M.A.M is supported by the program Intensificación de la Actividad Investigadora, from ISCIII-MICIN and Agencia Laín Entralgo, (CM).

References

[1] R. Janssen, L. Nijtmans, L. van den Heuvel, J. Smeitink, Mitochondrial complex I: structure, function and pathology, J. Inherit. Metab. Dis. 29 (2006) 499–515.
[2] O. Zhuchenko, M. Wehnert, J. Bailey, Z.S. Sun, C.C. Lee, Isolation, mapping, and genomic structure of an X-linked gene for a subunit of human mitochondrial complex I, Genomics 37 (1996) 281–288.
[3] H.C. Au, B.B. Seo, A. Matsuno-Yagi, T. Yagi, I.E. Scheffler, The *NDUFA1* gene product (MWFE protein) is essential for activity of complex I in mammalian mitochondria, Proc. Natl Acad. Sci. U. S. A. 96 (1999) 4354–4359.

[4] N. Yadava, P. Potluri, E.N. Smith, A. Bisevac, I.E. Scheffler, Species specific and mutant MWFE proteins. Their effect on the assembly of a functional mammalian mitochondrial complex I, J. Biol. Chem. 277 (2002) 21221–21230.
[5] N. Yadava, T. Houchens, P. Potluri, I.E. Scheffler, Development and characterization of a conditional mitochondrial complex I assembly system, J. Biol. Chem. 279 (2004) 12406–12413.
[6] R. Chen, I.M. Fearnley, S.Y. Peak-Chew, J.E. Walker, The phosphorylation of subunits of complex I from bovine heart mitochondria, J. Biol. Chem. 279 (2004) 26036–26045.
[7] B. Schilling, R. Aggeler, B. Schulenberg, J. Murray, R.H. Row, R.A. Capaldi, B.W. Gibson, Mass spectrometric identification of a novel phosphorylation site in subunit NDUFA10 of bovine mitochondrial complex I, FEBS Lett. 579 (2005) 2485–2490.
[8] N. Yadava, P. Potluri, I.E. Scheffler, Investigations of the potential effects of phosphorylation of the MWFE and ESSS subunits on complex I activity and assembly, Int. J. Biochem. Cell Biol. 40 (2008) 447–460.
[9] J.A.M. Smeitink, L.W. van den Heuvel, S. DiMauro, The genetics and pathology of oxidative phosphorylation, Nat. Rev. Genet. 2 (2001) 342–352.
[10] W. Koopman, S. Verkaart, H.J. Visch, S. van Emst-de Vries, L. Nijtmans, J. Smeitink, P. Willems, Human NADH: ubiquinone oxidoreductase deficiency. Radical changes in mitochondrial morphology? Am. J. Physiol. Cell Physiol. 293 (2007) C22–C29.
[11] M. Lazarou, D.R. Thornburn, M.T. Ryan, M. McKenzie, Assembly of mitochondrial complex I and defects in disease, Biochim. Biophys. Acta 1793 (2009) 78–88.
[12] F. Distelmaier, W.J.H. Koopman, L. van den Heuvel, R.J. Rodenburg, E. Mayatepek, P.H.G.M. Willems, A.M. Smeitink, Mitochondrial complex I deficiency: from organelle dysfunction to clinical disease, Brain 132 (pt4) (2009) 833–842.
[13] A. Iuso, S. Scacco, C. Piccoli, F. Bellomo, V. Petruzzella, R. Trentadue, M. Minuto, M. Ripoli, N. Capitanio, M. Zeviani, S. Papa, Dysfunctions of cellular oxidative metabolism in patients with mutations in the NDUFS1 and NDUFS4 genes of complex I, J. Biol. Chem. 281 (2006) 10374–10380.
[14] S. Verkaart, W.J.H. Koopman, S.E. van Emst-de Vries, L.G.J. Nijtmans, W.P.J. van den Heuvel, J.A.M. Smeitink, P.H.G.M. Willems, Superoxide production is inversely related to complex I activity in inherited complex I deficiency, Biochim. Biophys. Acta 1772 (2007) 373–381.
[15] S. Verkaart, W.J.H. Koopman, J. Cheek, S.E. van Emst-de Vries, L.G.J. Nijtmans, W.P.J. van den Heuvel, J.A.M. Smeitink, P.H.G.M. Willems, Mitochondrial and cytosolic thiol redox state are not detectably altered in isolated human *NADH:ubiquinone oxidoreductase deficiency*, Biochim. Biophys. Acta 1772 (2007) 1041–1051.
[16] G. Benard, N. Bellance, D. James, P. Parrone, H. Fernández, T. Letellier, R. Rossignol, Mitochondrial bioenergetics and structural network organization, J. Cell Sci. 120 (2007) 838–848.
[17] N. Pham, T. Richardson, J. Cameron, B. Chue, B.H. Robinson, Altered mitochondrial structure and motion dynamics in living cells with energy metabolism defects revealed by real time microscope imaging, Microsc. Microanal. 10 (2004) 247–260.
[18] W. Koopman, H.J. Visch, S. Verkaart, L. van den Heuvel, J. Smeitink, P. Willems, Mitochondrial network complexity and pathological decrease in complex I activity are tightly correlated in isolated human complex I deficiency, Am. J. Physiol. Cell Physiol. 289 (2005) 881–890.
[19] O. Guillery, F. Malka, P. Frachon, D. Milea, M. Rojo, A. Lombès, Modulation of mitocondrial morphology by bioenergetics defects in primary human fibroblasts, Neuromusc. Dis. 18 (2008) 319–330.
[20] M. Martínez-Díez, G. Santamaría, A.D. Ortega, J.M. Cuezva, Biogenesis and dynamics of mitochondria during the cell cycle: significance of 3′ UTRs, PLoS One 1 (2006) e107.
[21] D.C. Chan, Mitochondrial dynamics in disease, N. Engl. J. Med. 356 (2007) 1707–1709.
[22] G. Benard, R. Rossignol, Mitochondrial fluidity matters. Focus on, inherited complex I deficiency is associated with faster protein diffusion in the matrix of moving mitochondria, Am. J. Physiol. Cell Physiol. 294 (2008) C1123.
[23] S. Duvezin-Caubet, R. Jagasia, J. Wagener, S. Hofmann, A. Trifunovic, A. Hansson, A. Chomyn, M.F. Bauer, G. Attardi, N.G. Larsson, W. Neupert, A.S. Reichert, Proteolytic processing of OPA1 links mitochondrial dysfunction to alterations in mitochondrial morphology, J. Biol. Chem. 281 (2006) 37972–37979.
[24] O. Guillery, F. Malka, T. Landes, E. Guillou, C. Blakcstone, A. Lombés, P. Belenguer, D. Arnoult, M. Rojo, Metalloprotease-mediated OPA1 processing is modulated by the mitochondrial membrane potential, Biol. Cell 100 (2008) 315–325.
[25] D. Fernández-Moreira, C. Ugalde, R. Smeets, R.J.T. Rodenburg, E. Lopez-Laso, M.L. Ruiz-Falcó, P. Briones, M.A. Martín, J.A.M. Smeitink, J. Arenas, X-linked NDUFA1 gene mutations associated with mitochondrial encephalomyopathy, Ann. Neurol. 61 (2007) 73–83.
[26] B. Martínez, P. del Hoyo, M.A. Martín, J. Arenas, A. Pérez-Castillo, A. Santos, Thyroid hormone regulates oxidative phosphorylation in the cerebral cortex and striatum of neonatal rats, J. Neurochem. 78 (2001) 1054–1063.
[27] A.L. Andreu, R. Martínez, R. Martí, E. García-Arumi, Quantification of mitocondrial DNA copy number: pre-analytical factors, Mitochondrion 9 (2009) 242–246.
[28] F. López-Ríos, M. Sánchez-Aragó, E. García-García, A.D. Ortega, J.R. Berrendero, F. Pozo-Rodríguez, A. López-Encuentra, C. Ballestín, J.M. Cuezva, Loss of the mitochondrial bioenergetic capacity underlies the glucose avidity of carcinomas, Cancer Res. 67 (2006) 9013–9017.
[29] D.A. Bass, J.W. Parce, L.R. Dchatelet, P. Szejda, M.C. Seeds, M. Thomas, Flow cytometric studies of oxidative product formation by neutrophils: a graded response to membrane stimulation, J. Immunol. 130 (1983) 1910–1917.
[30] M.M. Bradford, A rapid and sensitive method for the quantitation of microgram quantities of protein utilizing the principle of protein–dye binding, Anal. Biochem. 72 (1976) 248–254.
[31] R. Rossignol, R. Gilkerson, R. Aggeler, K. Yamagata, S.J. Remington, R.A. Capaldi, Energy substrate modulates mitochondrial structure and oxidative capacity in cancer cells, Cancer Res. 64 (2004) 985–993.
[32] P. de Lonlay, C. Mugnier, D. Sanville, K. Chantrel-Groussard, P. Bénit, S. Lebon, D. Chrétien, N. Kadhom, S. Saker, G. Gyapay, S. Romana, J. Weissenbach, A. Munnich, P. Rustin, A. Rötig, Cell complementation using Genebridge 4 human: rodent hybrids for physical mapping of novel mitochondrial respiratory chain deficiency genes, Hum. Mol. Genet. 11 (2002) 3273–3281.
[33] M. Wu, A. Neilson, A.L. Swift, R. Moran, J. Tamagnine, D. Parslow, S. Armistead, K. Lemire, J. Orrell, J. Teich, S. Chomicz, D.A. Ferrick, Multiparameter metabolic analysis reveals a close link between attenuated mitochondrial bioenergetic function and enhanced glycolysis dependency in human tumour cells, Am. J. Physiol. Cell Physiol. 292 (2007) C125–C136.
[34] E. Gnaiger, Capacity of oxidative phosphorilation in human skeletal muscle, new perspectives of mitochondrial physiology, Int. J. Biochem. Cell Biol. 41 (2009) 1837–1845.
[35] A. Hansson, N. Nicole, E. Dufour, A. Rantanen, K. Hultenby, D.A. Clayton, R. Wiborn, N.G. Larsson, A switch in metabolism precedes increased mitochondrial biogenesis in respiratory chain-deficient mouse hearts, PNAS 101 (2004) 3136–3141.
[36] F. Pallotti, A. Baracca, E. Hernández-Rosa, W.F. Walker, G. Solaini, G. Lenaz, G.V. Melzi D'Eril, S. Dimauro, E.A. Schon, M.M. Davidson, Biochemical analysis of respiratory function in cybrid cell lines harbouring mitochondrial DNA mutations, Biochem. J. 384 (2004) 287–293.
[37] G. Santamaría, M. Martínez-Díaz, I. Fabregat, J.M. Cuezva, Efficient execution of cell death in non-glycolytic cells requires the generation of ROS induced by the activity of mitochondrial H^+-ATP synthase, Carcinogenesis 27 (2006) 925–935.
[38] P. Potlury, A. Davila, E. Ruiz-Pesini, D. Mishmar, S. O'Hearn, S. Hancock, M. Simon, I.E. Scheffler, D.C. Wallace, V. Procaccio, A novel NDUFA1 mutation leads to a progressive mitochondrial complex-I-specific neurodegerative disease, Mol. Genet. Metab. 96 (2009) 189–195.
[39] P.H.G.M. Willems, J.A.M. Smeitink, W.J.H. Koopman, Mitochondrial dynamics in human NADH: ubiquinone oxidoreductase deficiency, Int. J. Biochem. Cell Biol. 41 (2009) 1773–1782.
[40] J. Caissereau, A. Chevrollier, N. Gueguen, M.C. Malinge, F. Letournel, G. Nicolas, L. Richard, M. Ferre, C. Verny, F. Dubas, V. Procaccio, P. Amati-Bonneau, D. Bonneau, P. Reynier, Mitochondrial Complex I deficiency in GDAP1-related autosomal dominant Charcot–Marie–Tooth disease (CMT2K), Neurogenetics 10 (2009) 145–150.
[41] B.J. Hanson, R.A. Capaldi, M.F. Marusich, S.W. Sherwood, An inmunocytochemical approach to detection of mitochondrial disorders, J. Histochem. Cytochem. 50 (2002) 1281–1288.
[42] C. Chinopoulos, V. Adam-Vizi, Mitochondria as ATP consumers in cellular pathology, Biochim. Biophys. Acta 1802 (2010) 221–227.
[43] L.J. Reitzer, B.M. Wice, D. Kennell, Evidence that glutamine, not sugar, is the major energy source for cultured HeLa cells, J. Biol. Chem. 254 (1979) 2669–2676.
[44] J.A. Enriquez, J. Cabezas-Herrera, M.P. Bayona-Bafaluy, G. Attardi, Very rare complementation between mitochondria carrying different mitochondrial DNA mutations points to intrinsic genetic autonomy of the organelles in cultures human cells, J. Biol. Chem. 275 (2000) 11207–11215.
[45] B.H. Robinson, R. Petrova-Benedict, J.R. Buncic, D.C. Wallace, Nonviability of cells with oxidative defects in galactose medium: a screening test for affected patient fibroblasts, Biochem. Med. Metab. Biol. 48 (1992) 122–126.
[46] K. Auré, K. Mamchaoui, P. Frachon, G.S. Butler-Browne, A. Lombés, V. Mouly, Impact on oxidative phosphorylation of immortalization with the telomerase gene, Neuromuscul. Disord. 17 (2007) 368–375.
[47] G. Benard, R. Rossignol, Ultrastructure of the mitochondrion and its bearing on function and bioenergetics, Antioxid. Redox Signal. 10 (2008) 1313–1342.
[48] L. Plecitá-Hlavatá, M. Lessard, J. Santorová, J. Bewersdorf, P. Jezek, Mitochondrial oxidative phosphorylation and energetic status are reflected by morphology of mitochondrial network in INS-1E and HEP-G2 cells viewed by 4Pi microscopy, Biochim. Biophys. Acta 1777 (2008) 834–846.
[49] G. Twig, B. Hyde, O.S. Shirihai, Mitochondrial fusion, fission and autophagy as a quality control axis: the bioenergetic view, Biochim. Biophys. Acta 1777 (2008) 1902–1907.
[50] F. Distelmaier, H.-J. Visch, J.A.M. Smeitink, E. Mayapetek, W.J.H. Koopman, P.H.G.M. Willems, The antioxidant Trolox restores mitochondrial membrane potential and Ca^{2+}-stimulated ATP production in human complex I deficiency, J. Mol. Med. 87 (2009) 515–522.
[51] F. Legros, A. Lombès, P. Frachon, M. Rojo, Mitochondrial fusion in human cells is efficient, requires the inner membrane potential, and is mediated by mitofusins, Mol. Biol. Cell 13 (2002) 4343–4354.
[52] M.P. Murphy, How mitochondria produce reactive oxygen species, Biochem. J. 417 (2009) 1–13.